# PREPARATION AND CHARACTERISTICS OF POLYURETHANE-BASED COMPOSITES REINFORCED WITH BIOACTIVE CERAMICS

Natalia Złocista-Szewczyk, Piotr Szatkowski [iD],
Kinga Pielichowska* [iD]

AGH University of Science and Technology,
Faculty of Materials Science and Ceramics,
Department of Biomaterials and Composites,
al. A. Mickiewicza 30, 30-059 Kraków, Poland
*e-mail: kingapie@agh.edu.pl

## Abstract

*The purpose of the study was to synthesize and characterize a series of porous polyurethane-based composites modified with β-tricalcium phosphate (TCP) and hydroxyapatite (HAp). The composites were obtained by the one-step bulk polyaddition method using poly(ethylene glycol) (PEG) as a soft segment, 4,4'-diphenylmethane diisocyanate (MDI), 1,4-butanediol (BDO) as a chain extender and selected bioactive bioceramics. The obtained composites were characterized using FTIR, DSC, TG and SEM/EDX methods. Moreover, in vitro chemical stability and wettability tests were performed. The preliminary assessment of mechanical properties, porosity and in vitro chemical stability was performed. The test results showed that the best pore distributions, as well as Young's modulus, were found for the hydroxyapatite-modified composites and PU/20% TCP. The wettability investigations revealed that the contact angle of PU composites was in the range 50-80°, which indicates the hydrophobic nature of the materials. The in vitro biostability studies confirmed that all tested composites were chemically stable during incubation in the simulated body fluid. By using infrared spectroscopy the presence of urethane bonds and completion of reaction were evidenced. The results showed that the bioactivity of the materials was improved, which makes good perspectives for the obtained materials to be considered as potential scaffolds in bone tissue regeneration.*

***Keywords****: polyurethane, HAp, TCP, orthopaedics, bone regeneration*

## Introduction

One of the observed trends in the development of medicine is the biomimetic approach. Currently, studies are performed on materials imitating human tissues, such as bone. Different types of materials and implants not only perform mechanical functions but also facilitate the regeneration of damaged tissues.

The bone tissue can be considered as a nanocomposite of an organic collagen matrix, reinforced with an inorganic phase - hydroxyapatite (HAp). Having been damaged, the bone tissue exhibits a very high self-healing ability. However, there is a critical size of the loss which the bone is not able to heal properly [1-3]. Resorbable polymers are most commonly used as they can stabilize the damaged tissue and then degrade in the body. During the gradual resorption, they simultaneously release the medicaments, such as antibiotics or proteins [1,4]. One of the most promising polymers for bone tissue regeneration are polyurethanes (PU). Polyurethane-based materials for bone tissue regeneration and replacement have been widely studied in recent years. Hence, in the work by Gabard et al. [5], PU modified with HAp nanocrystals was described. They showed that the addition of nanoHAp reduced the surface energy of the material, which made it possible to control the initial absorption of the protein and simultaneously inhibit the spread of inflammatory cells. The tests confirmed the material's high decomposition temperature, which enables the proper sterilization. Biological studies revealed biocompatibility in both in vitro and in vivo conditions. The foam composite made of PU modified with bioglass was investigated by Ryszkowska et al. [6]. The porosity of the obtained composite meets the requirements for bone tissue engineering. Additionally, the material has a high biological activity, which was confirmed by incubation in the simulated body fluid (SBF) when apatites were formed on the foam surface. Dulińska-Molak et al. [7] studied PU filled with calcite composites. They found that ceramic composites based on polyurethanes exhibited better properties as implants than the unfilled materials. The results showed that calcium carbonate particles improved the properties of composites, such as biostimulation or adhesion capacity. In addition, fillers such as calcite and argonite were compared. Studies revealed that despite the smaller particle diameter and more uniform distribution in the PU matrix, the composite with argonite showed worse properties than those with calcite. In the work of Das et al. [8] a composite consisting of vegetable-oil-based hyperbranched polyurethane and rapeseed protein functionalized multi-walled carbon nanotubes was prepared. The results showed that the obtained composite rebuilt the bone in 93% after only 45 days. Composites made of polyurethanes and bioactive ceramics show some similarities to human bones. The HAp chemical structure is very similar to the mineral part of bone. The polymer matrix ensures adequate flexibility, hardness and compressive strength [9]. In addition, ceramic nanoparticles in the polymer matrix have good adhesion [10]. HAp is also responsible for bioactivity, which results in forming the apatite layer through ion-exchange reactions [9,10]. Another application of polyurethane foams is the development of composite bones. The PU foam structure resembles spongy bone, therefore, in order to restore the bone structure, the polyurethane foam was coated with the glass fibre reinforced epoxy resin to mimic the cortical bone. This composite exhibits very similar fatigue properties, Young's modulus, strength and hardness to natural bone [11,12].

The main goal of our research was to design and study the biodegradable PU-based composite scaffolds filled with β-TCP microparticles and hydroxyapatite (HAp) which can be applied as biomaterials in bone tissue engineering. The influence of β-TCP and HAp on mechanical and thermal properties, porosity, biodegradability and bioactivity of PU-based scaffolds was investigated.

## Materials and Methods

### Preparation of porous polyurethane-based composites

4,4'-diphenylmethane diisocyanate (MDI), poly(ethylene glycol) (PEG) with an average molar mass 2000 g/mol and 1,4-butanediol (BDO) were obtained from Sigma Aldrich company. β-TCP and HAp microparticles were produced by Fluka Chemie GmbH. It was assumed that the resulting foam should contain 40% of the soft segments (PEG). For this purpose, appropriate calculations were made and the amounts of substrates used are shown in TABLE 1.

$$m_{PEG} = x \cdot m_{PU}$$

where:
$m_{PEG}$ - PEG mass [g],
x - PEG content,
$m_{PU}$ - PU mass [g].

$$m_{MDI} = (m_{PU} - m_{PEG}) - m_{BDO}$$
$$R = M_i / f_i$$
$$m_{MDI} / R_{MDI} = m_{PEG} / R_{PEG} + m_{BDO} / R_{BDO}$$

where:
$m_{MDI}$, $m_{PEG}$, $m_{BDO}$, $m_{PU}$ - masses of MDI, PEG, BDO and PU, respectively, [g]
$R_{MDI}$, $R_{PEG}$, $R_{BDO}$ - equivalents of MDI, PEG, BDO, respectively, [g/mol]
$M_{MDI}$, $M_{PEG}$, $M_{BDO}$ - molar mass, respectively: MDI, PEG, BDO, [g/mol]
$f_{MDI}$, $f_{PEG}$, $f_{BDO}$ - number of active functional groups: MDI, PEG, BDO, respectively.

Polyurethanes were foamed using water. Polyurethane composite materials were obtained using the one-step bulk polyaddition method. In the first step, PEG was dried at the temperature 60-70°C under vacuum. Next, the proper amount of melted PEG was mixed with the TCP or HAp by sonication. The appropriate amounts of BDO and water were then added and mixed mechanically. Then the isocyanate was melted and preheated up to at 55-60°C and added into the previously prepared mixture. The reaction mixture was stirred intensively for one minute and next the foam growing was observed. Finally, the obtained foams were heated and conditioned for 24 h at 50°C.

The FTIR measurements were performed using a VARTEX 70 spectrometer, with the ATR attachment with diamond crystal, at room temperature in the range of 4000-550 cm$^{-1}$ and at the 2 cm$^{-1}$ resolution. The porosity was determined planimetrically, using the VHX 5000 digital microscope.

The DSC tests were performed using the DSC 1 differential scanning calorimeter from METTLER TOLEDO. The samples for DSC with mass ca. 4 ± 0.1 mg were placed in closed and pierced aluminium pans. The measurements were taken at the 10°C/min heating rate under a nitrogen atmosphere with the 30 ml/min flow rate. At the beginning the samples were heated form -90° up to 200°C, then cooled to -70°C and again heated up to 200°C.

The mechanical tests (static compression) were performed using ZWICK machine, in accordance with ISO 3167 on the cubic samples with dimensions 10x10x10 mm and at 2 mm/min speed. The results were the mean of three measurements.

The surface wettability analysis was performed using the DSA10 automatic drop analysis system. The obtained results are the mean of 5 measurements of distilled water drops with 15-25 μl volume range.

**TABLE 1. Quantitative proportions of substrates for PU composites synthesis.**

| TCP [%] | PEG [g] | MDI [g] | BDO [g] | TCP [g] |
|---|---|---|---|---|
| 0 | | | | - |
| 2.5 | | | | 0.5 |
| 5 | 8 | 10.45 | 2.91 | 1 |
| 10 | | | | 2 |
| 20 | | | | 4 |
| HAp [%] | PEG [g] | MDI [g] | BDO [g] | HAp [g] |
| 0 | | | | - |
| 2.5 | | | | 0.5 |
| 5 | 8 | 10.45 | 2.91 | 1 |
| 10 | | | | 2 |
| 20 | | | | 4 |

The chemical stability of the materials was determined by changes in pH and ionic conductivity of the water extracts in accordance with EN ISO 10993-13. The samples were placed in plastic containers with the sample to water ratio 1:10, and incubated for 8 weeks at 37°C. The pH and conductivity were measured each week.

The preliminary bioactivity assessment was performed in the simulated body fluid (SBF). The samples were incubated for 21 days at the constant temperature of 37°C, the SBF was replaced every 3 days. The changes occurring on the surface of the samples were observed using NOVA NANO SEM 200 scanning electron microscope equipped with EDAX EDS analyzer.

## Results and Discussions

The FTIR spectra for obtained PUR composites are presented in FIG. 1.

In the unmodified polyurethane sample, the absorption bands were observed in the range of 3450-3300 cm$^{-1}$, which was characteristic for the N-H group stretching vibrations. The bands in the range of about 2900 cm$^{-1}$ derived from stretching vibrations typical for CH$_2$. They were also present in the spectra of PU composites. At about 1520 cm$^{-1}$ there were bands derived from secondary amide groups, and at 1240 cm$^{-1}$ from the tertiary. The obtained results confirmed forming the urethane bonds during the polyurethane synthesis. In the range of about 1160-1040 cm$^{-1}$ there was the triplet derived from the stretching vibrations of the C-O-C group in PEG [13].

With the addition of TCP, an increase in the band intensity around 1040, 600 and 550 cm$^{-1}$ was observed. These were typical bands derived from the stretching and bending vibrations of PO$_4^{3-}$. An increase in the band intensity at 1040 cm$^{-1}$ may be attributed to the overlapping of C-O-C group and those characteristic for the phosphate group originating from TCP. The absorption bands at ca. 1700 cm$^{-1}$ came from the carbonyl group. There were no bands from isocyanate groups at ca. 2270 cm$^{-1}$ that confirmed the complete reaction of isocyanate groups [13,14]. Moreover, for the composites with HAp no absorption bands from OH group at 3571 cm$^{-1}$ were observed that suggest the chemical bonding of HAp with PU chains.
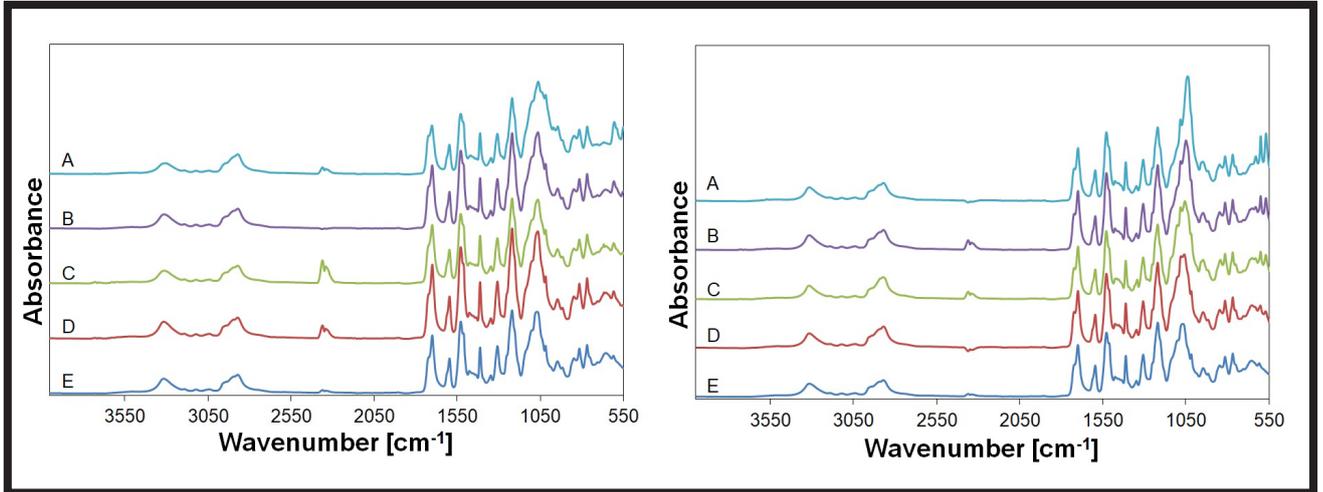
**FIG. 1. FTIR spectra for PU composites with TCP (left) and HAp (right): A) 0%, B) 2.5%, C) 5%, D) 10%, E) 20%.**
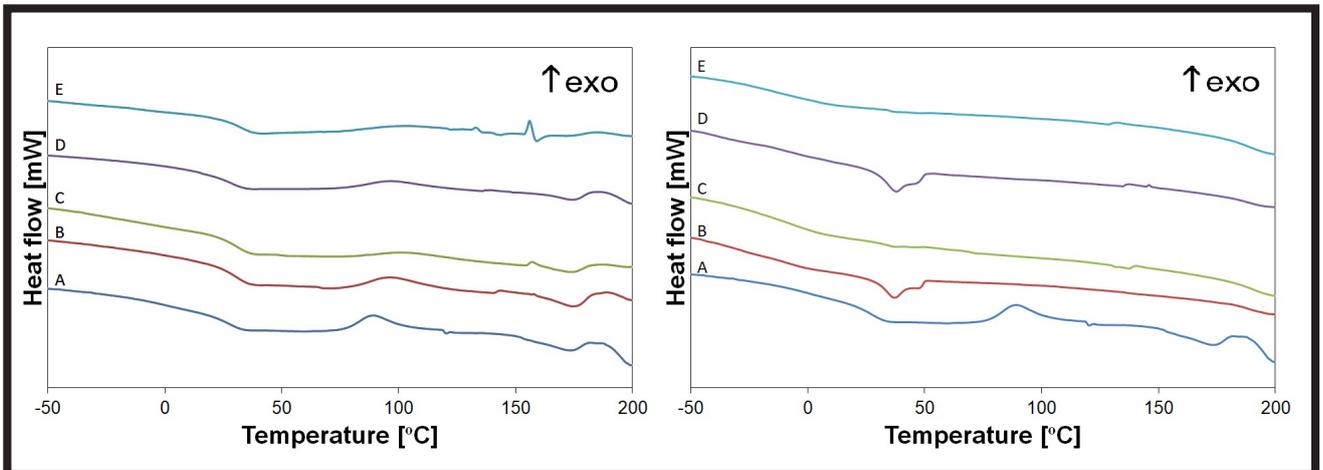


**FIG. 2. DSC curves from the second heating for PU composites with HAp (left) and TCP (right): A) 20%, B) 10%, C) 5%, D) 2.5%, E) 0%.**

**TABLE 2. DSC results: the melting temperature, glass transition and heat of fusion of obtained PU and PU composites.**

| Sample | Glass transition of soft segments | | Glass transition of hard segments | | Melting of soft segments | | Cold crystallization | | Melting of hard segments | |
|---|---|---|---|---|---|---|---|---|---|---|
| | $T_g$ [°C] | $\Delta C_p$ [kJ/molK] | $T_g$ [°C] | $\Delta C_p$ [kJ/molK] | $T_{max}$ [°C] | Heat of fusion [J/g] | $T_{max}$ [°C] | Heat of crystalliza-tion [J/g] | $T_{max}$ [°C] | Heat of fusion [J/g] |
| PU | -14 | 0.086 | 29 | 0.235 | - | - | 89 | 4.7 | 174 | 1.6 |
| PU+2.5%HAp | -35 | 0.362 | 30 | 0.174 | 48 | - | - | - | - | - |
| PU+5%HAp | -12 | 0.498 | 35 | 0.055 | - | - | - | - | - | - |
| PU+10%HAp | -10 | 0.093 | 33 | 0.267 | 48 | - | - | - | - | - |
| PU+20%HAp | -21 | 0.456 | - | - | - | - | - | - | - | - |
| PU+2.5%TCP | - | - | 30 | 0.345 | - | - | 96 | 5.6 | 175 | 4.5 |
| PU+5%TCP | - | - | 31 | 0.319 | - | - | 103 | 4.4 | 174 | 1.7 |
| PU+10%TCP | - | - | 27 | 0.328 | - | - | 97 | 5.0 | 175 | 2.0 |
| PU+20%TCP | - | - | 31 | 0.248 | - | - | - | - | - | - |

The DSC curves of the obtained composites are shown in FIG. 2 and the results are summarized in TABLE 2.

The DSC curves analysis of the unmodified polyurethane revealed two glass transitions: the first one at -13.6ºC with a $\Delta Cp$ equal to 0.086 kJ/molK derived from the soft segments, and the second one at 29.7ºC with a $\Delta Cp$ of 0.235 kJ/molK originating from the hard segments. Next, at 89ºC a broad exothermic peak was observed that could be attributed to the cold crystallization. The melting of hard segments was observed at ca. 160ºC. Analysing the DSC curves of the samples containing HAp, it was revealed that the glass transition of soft segments ranged from -35°C to -10ºC depending on the amount of HAp. Moreover, the incorporation of HAp only slightly changed the glass temperature of the hard segments.

For the composites with 2.5% and 10% HAp, the melting temperature of the soft segments was 48.3°C and 47.9ºC, respectively. This effect overlapped the changes in the baseline derived from the glass transition of the hard segments. Melting of the hard segments in the PU/HAp composites was not observed.

For the PU with TCP the glass transition temperatures for the hard segments were close to those of the samples containing HAp. The PU/TCP samples showed neither the glass transition for the soft segments nor their melting. On the other hand, the cold crystallization and melting were observed for the hard segments at a level similar to the unmodified polyurethane.

FIG. 3 presents the PU composites microphotographs and FIGs. 4-6 the pore size distribution in the PU composites.
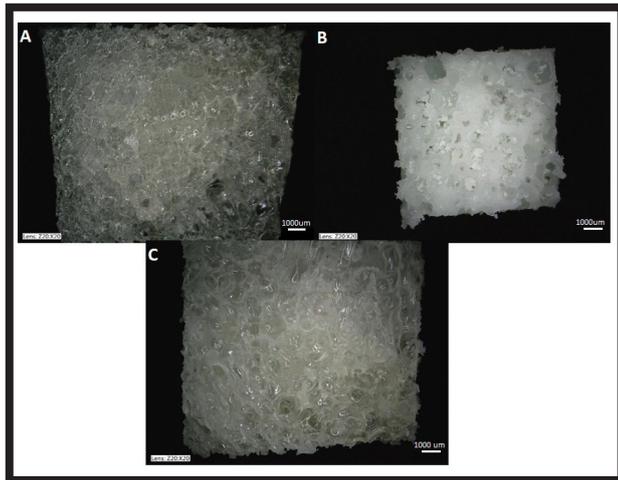


**FIG. 3. Microphotographs of PU composites: unmodified PU (A), PU/10% HAp (B) and 10% TCP (C).**
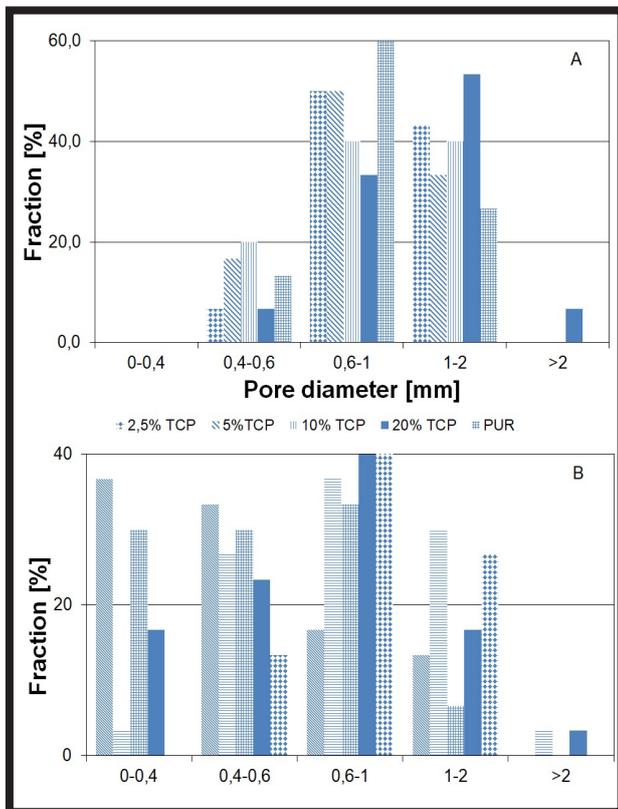


**FIG. 4. Pore size distribution in composites with TCP (A) and HAp (B).**
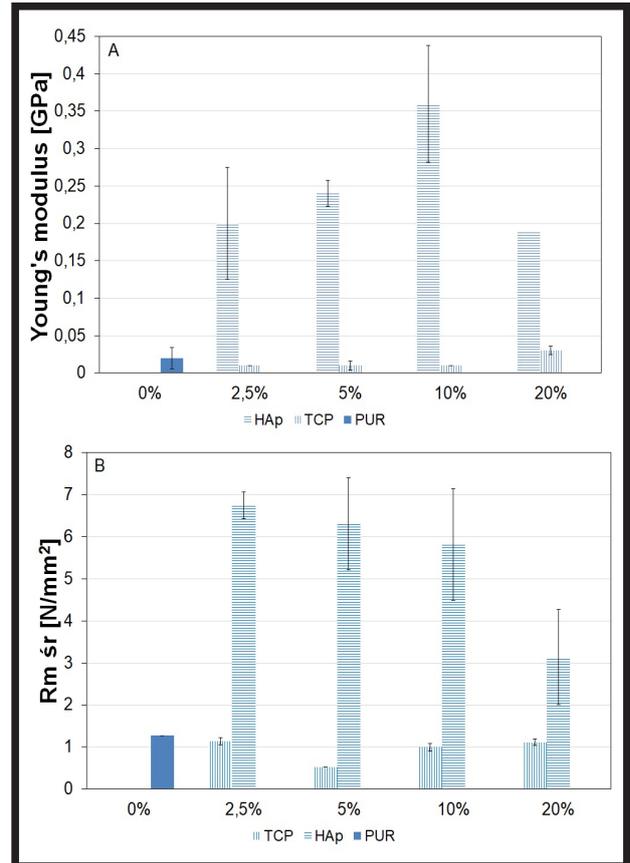


**FIG. 5. Young's modulus for PUR with HAp, TCP (A) and compression strength for PU composites (B).**
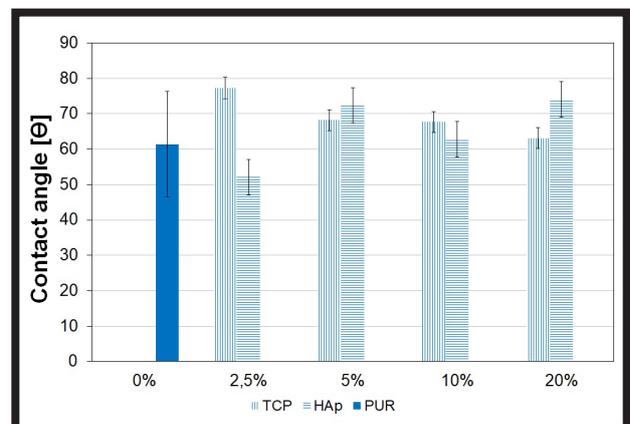


**FIG. 6. Contact angle values for the samples tested.**
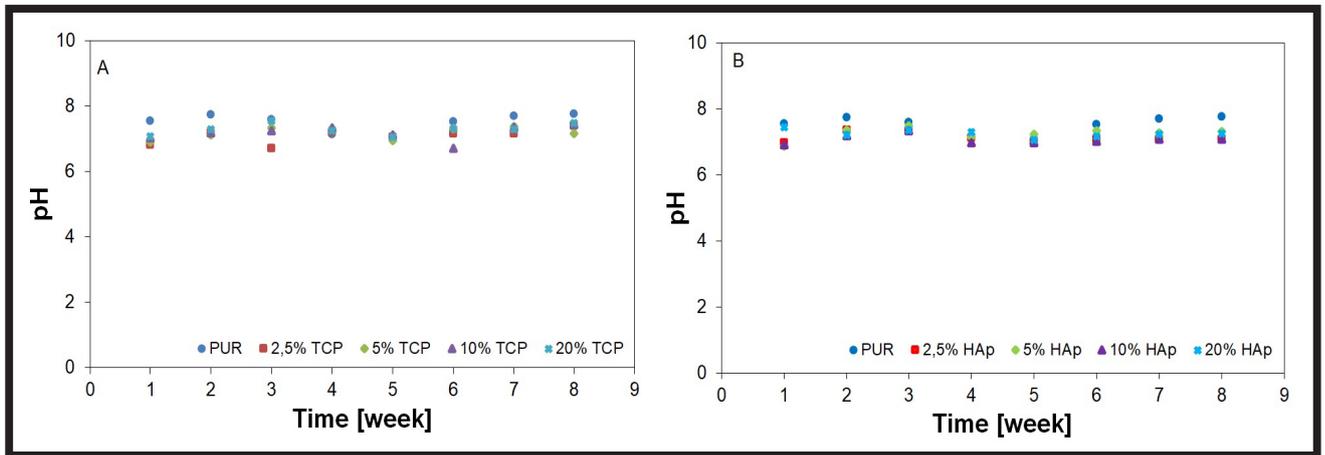
**FIG. 7. pH vs. incubation time for PU/TCP (A) and PU/HAp (B) composites.**
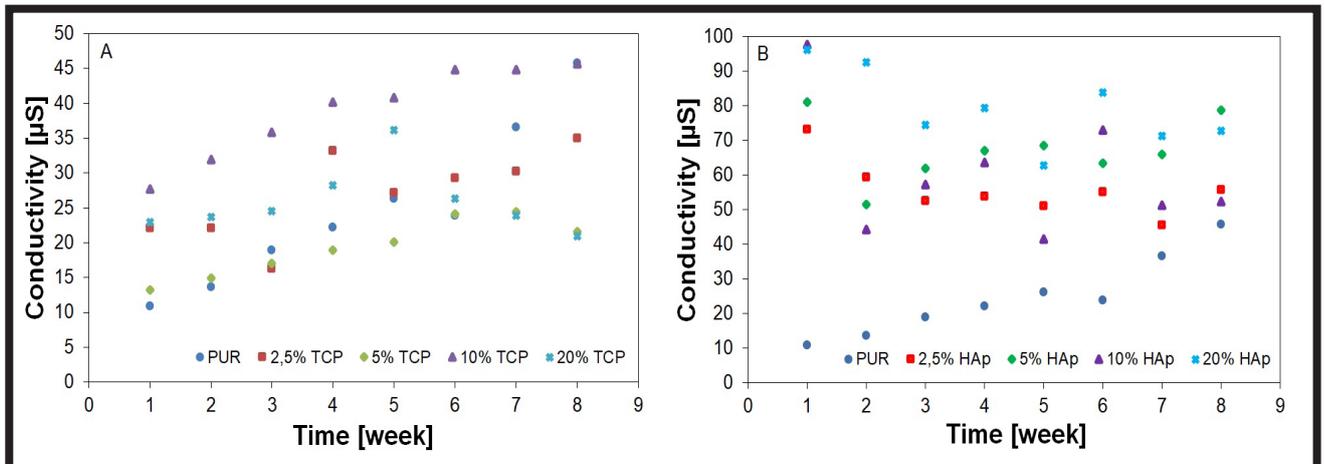


**FIG. 8. Conductivity vs. incubation time for PU/TCP (A) and PU/HAp (B) composites.**

The composites with TCP revealed a higher number of pores with larger diameters, which is favourable for osteointegration. The highest number of pores in the 0-0.5 mm range was observed in the 10% TCP composite. In the PU/HAp composites, a high number of small pores was observed. The HAp incorporation significantly influenced the pore size distribution, even at the small Hap amount (2.5wt%), while the TCP incorporation led to significant changes in pore sizes at the higher TCP contents (20wt%). In all the samples, pores of 0.4-0.6 mm diameter were observed. Most of the smallest pores were observed in the PU/2.5% HAp. It can be concluded that the most favourable microstructure and pore size distribution was found in the PU/HAp composites [13,14].

In the next step, the mechanical properties were investigated. The compression tests results are presented in FIG. 7.

It was observed that only the addition of TCP did not change the PU composites compressive strength significantly. However, for the PU/HAp composites, the incorporation of 2.5% caused a significant increase in the compressive strength. Moreover, it was observed that the increasing HAp content resulted in the compressive strength decrease.

The wettability investigation showed that the contact angle of PU composites was in the range 50-80° - FIG. 6. In the case of the PU/TCP composites with the TCP content increasing, the contact angle diminished. On the other hand, for the PU/HAp composites, an opposite trend was observed.

During the incubation studies, the pH measurements showed that both the TCP and HAp incorporation only slightly decreased the pH of the unmodified PU and PU composites - FIG. 7. This effect can be explained by the slightly alkaline character of TCP and HAp. In the work by Szczepańczyk et al. the similar behaviour of the samples in the PBS and Ringer solutions was observed [13].

It can be seen that for the PU/TCP composites the highest conductivity of filtrates was observed for the PU/10% TCP - FIG. 8. Generally, the higher conductivity was observed for the PU composites when compared to the unmodified PU. With the bioceramics content increase, the conductivity increased due to the TCP and HAp slow dissolution.

In the next step, the preliminary assessment of bioactivity was performed using the Kokubo method [15]. Results of SEM-EDX observations are presented in FIGs. 9 and 10.

It was observed that the PU sample surface is strongly wrinkled and uneven with only sodium chloride crystals - no apatite crystals were found. Generally, the uniform distribution of TCP and HAp in the PU matrix was confirmed. In the PU/TCP composites, the apatites were not observed on the surface, and calcium phosphates were introduced as a filler. The PU/HAp composites revealed better bioactivity, a formation of the apatite layer was observed especially for the PU/5% Hap sample. This phenomenon can be explained by the nucleation effect of HAp on forming the apatite layer on the composite surface. A similar effect was observed by Szczepańczyk et al. [5,13] where incorporating HAp into the PU matrix increased the apatite formation in the SBF.
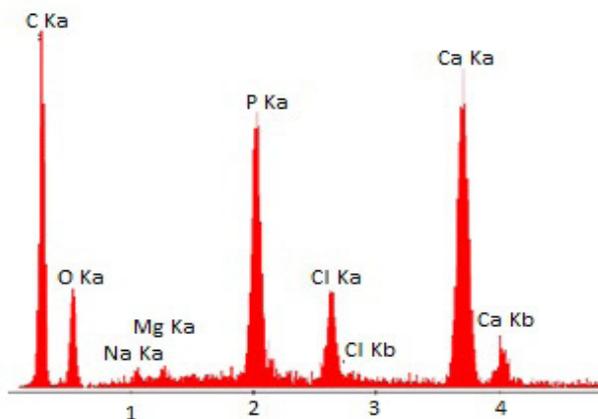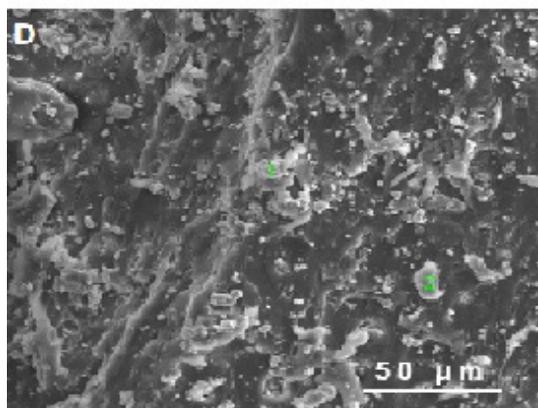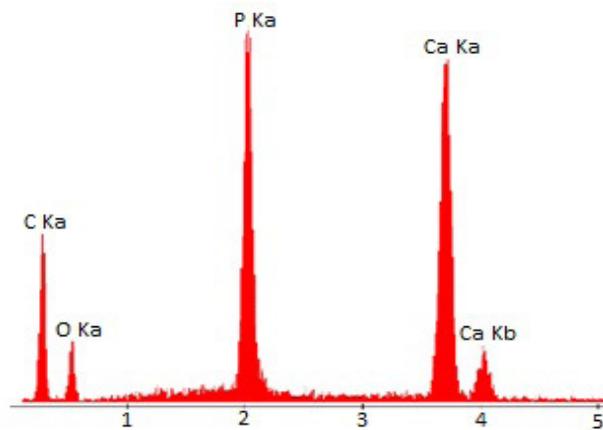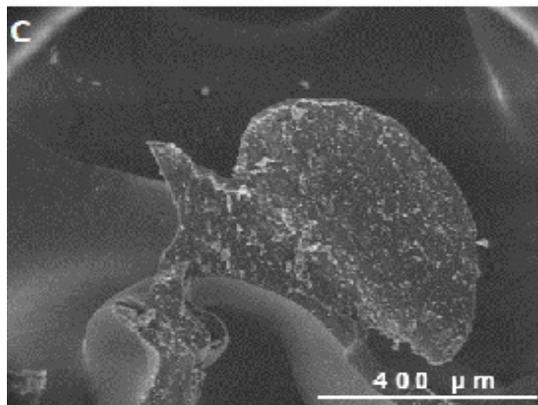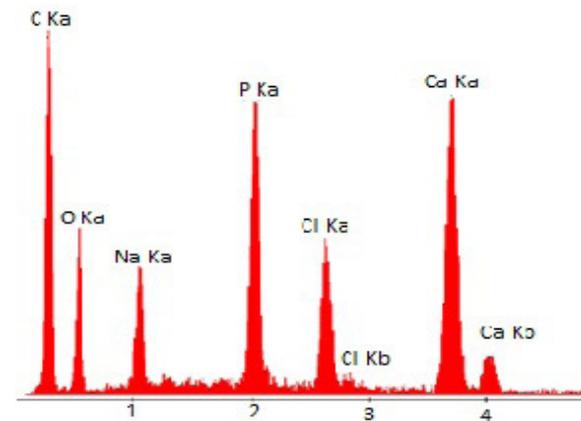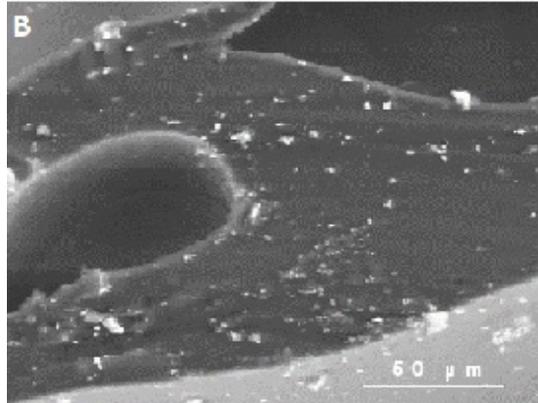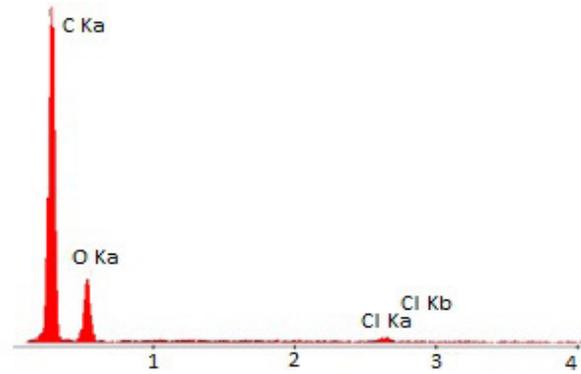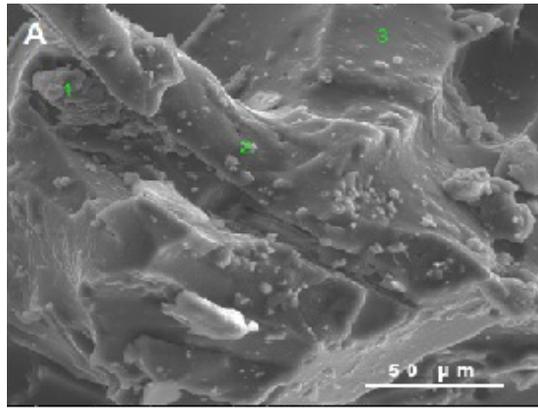
**FIG. 9. SEM microphotographs and EDS analysis results for PU with: A) 2.5%, B) 5%, C) 10%, D) 20% TCP after incubation in SBF.**
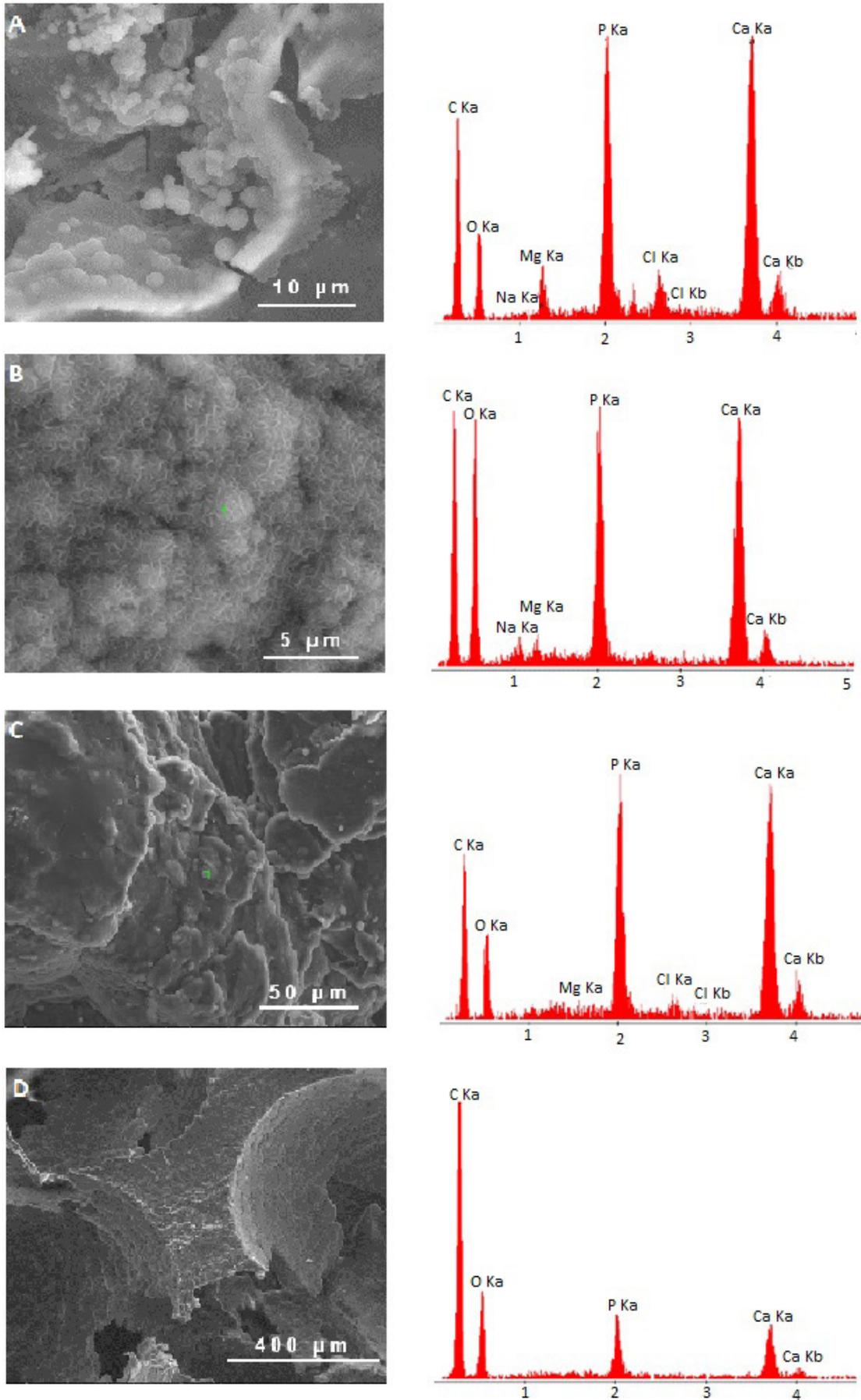
**FIG. 10. SEM microphotographs and EDS analysis results for PU with: A) 2.5%, B) 5%, C) 10%, D) 20% HAp after incubation in SBF.**

## Conclusions

In this work, the PU composites enhanced with TCP and HAp were obtained and characterized. The FTIR results confirmed the polyurethane structure and the complete polyaddition reaction. Moreover, for the HAp composites, the absorption bands from the OH group were not observed at 3571 cm$^{-1}$, which suggests the chemical bonding of HAp with the PU chains. The porosity investigations of the obtained materials showed that the best pore distribution was found in the PU/HAp and PU/20% TCP composites. The SEM observations confirmed the uniform distributions of fillers in the composites. Moreover, the PU/HAp composites exhibited better bioactivity. The mechanical tests showed an increase in Young's modulus of the samples with hydroxyapatite and 20% TCP content. The chemical stability assessment confirmed the good hydrolytical stability of the composites in distilled water. The composites only slightly affected the pH of the environment and pH changes did not exceed 7.0 ± 0.8. The conductivity increased with higher amounts of ceramic additives. The results proved that the obtained composites possess some potential in orthopaedics.

## Acknowledgements

### ORCID iDs

P. Szatkowski:  https://orcid.org/0000-0003-0861-6195
K. Pielichowska:  https://orcid.org/0000-0002-5049-8869

## References

[1] B. Świeczko-Żurek, A. Zieliński, i in.: Skrypt do przedmiotu biomateriały (2011).

[2] C. Turner and D. Burr: Experimental Techniques for Bone Mechanics, in Bone Mechanics Handbook, Second Edition, CRC Press (2001) 2-6.

[3] K.T. Łysiak-Drwal, Dominiak M., Malicka B.: Estimation of the influence of bone defects' dimensions on the healing outcome – 1-year observations. Stomatology 63 (2010) 365-376.

[4] B. Świeczko-Żurek: Biomateriały. Gdańsk (2009).

[5] L.P. Gabriel et al.: Bio-based polyurethane for tissue engineering applications: How hydroxyapatite nanoparticles influence the structure, thermal and biological behavior of polyurethane composites. Nanomedicine Nanotechnology, Biology and Medicine 13 (2017) 201-208.

[6] J.L. Ryszkowska, M. Auguścik, A. Sheikh, A.R. Boccaccini: Biodegradable polyurethane composite scaffolds containing Bioglass® for bone tissue engineering. Composite Science and Technology 70 (2010) 1894-1908.

[7] I. Dulińska-Molak, M. Lekka, K.J. Kurzydłowski: Surface properties of polyurethane composites for biomedical applications. Applied Surface Science 270 (2013) 553-560.

[8] B. Das et al.: Bio-functionalized MWCNT/hyperbranched polyurethane bionanocomposite for bone regeneration. Biomedical Materials 10 (2015) 1-16.

[9] J. Chlopek, P. Rosół, A. Morawska-Chochół: Durability of polymer-ceramics composite implants determined in creep tests. Composite Science and Technology 66 (2006) 1615-1622.

[10] K. Pielichowska: The influence of molecular weight on the properties of polyacetal/hydroxyapatite nanocomposites. Part 2. In vitro assessment. Journal of Polymer Research 19 (2012) 9788–1–9778–10.

[11] V. Shim and J. Boheme: Use of Polyurethane Foam in Orthopaedic Biomechanical Experimentation and Simulation (2012).

[12] A.R. Fariza, A. Zuraida, I. Sopyan: Application of Low Cost Polyurethane (PU) Foam for Fabricating Porous Tri-Calcium Phosphate (TCP). Journal of Biomimetics, Biomaterials, and Tissue Engineering 8 (2010) 1-7.

[13] P. Szczepańczyk, K. Pietryga, K. Pielichowska, J. Chłopek: Porous composites polyurethane/ß-TCP for orthopaedic applications. Engineering of Biomaterials 121 (2013) 33-41.

[14] M. Berdychowski: Zastosowanie modeli porowatych biomateriałów w procesach projektowania i symulacji (2014).

[15] T. Kokubo, H. Takadama: How useful is SBF in predicting in vivo bone bioactivity? Biomaterials 27 (2006) 2907-2915.